FIBRE-OPTIC SENSOR FOR SIMULTANEOUS MEASUREMENT OF THICKNESS AND REFRACTIVE INDEX OF LIQUID LAYERS

Marcin Marzejon[1, 2)], Katarzyna Karpienko[1)], Adam Mazikowski[1)], Małgorzata Jędrzejewska-Szczerska[1)]

1) *Gdańsk University of Technology, Faculty of Electronics, Telecommunications and Informatics,*
G. Narutowicza 11/12, 80-345 Gdańsk, Poland (marcin.marzejon@pg.edu.pl, ✉ katkarpi@pg.edu.pl,
+48 58 347 1584, adamazik@pg.edu.pl, malszcze@pg.edu.pl),
2) *Polish Academy of Sciences, Institute of Physical Chemistry, Kasprzaka 44/52, 01-224 Warsaw, Poland*

Abstract

In this paper, we present a fibre-optic sensor for simultaneous measurement of refractive index and thickness of liquid layers. We designed an experimental low-coherence setup with two broadband light sources and an extrinsic fibre-optic Fabry–Pérot interferometer acting as the sensing head. We examined how the refractive index of a liquid film and its thickness affect spectrum at the output of a fibre-optic interferometer. We performed a series of experiments using two light sources and only one sensing head. The spectra were collected in ranges of 1220÷1340 nm and 1500÷1640 nm. The obtained results show that using two spectra recorded simultaneously for two wavelength ranges enables to determine thickness in a range of 50÷500 μm, and refractive index of a liquid film in a range of 1.00÷1.41 RIU using only one sensing head.

Keywords: fibre-optic, sensors, interferometry, Fabry–Pérot interferometer.

1. Introduction

Fibre-optic sensors have several advantages in comparison with the non-fibre optoelectronic sensors. They are characterized by a very small size and small weight, and they often do not require contact with the measurand – enabling to perform non-invasive, point measurements. Another important advantage is the fact that they are non-conductive sensors, so they do not create a risk of an electric discharge. Also, using fibre-optic technology enables to develop distributed sensors, a network of multiplexed sensors or remote sensors. Because of all these features, fibre-optic sensors can be used for measurements in normally inaccessible areas and harsh environments (mines, oil wells, places exposed to chemically aggressive agents). Moreover, the use of modern nanomaterials in such sensors makes them well suited for bio-sensing [1–7].

Fibre-optic sensors are an important and growing field of science and technology. They are devices that enable to quantify parameters of the world around us. These sensors provide

information about the appearance of a particular stimulus, a certain threshold value, or the value of currently examined physical quantity.

Some of the most important groups of fibre-optic sensors are the refractive index sensors and the displacement sensors. They are the basis for indirect measurements of a wide range of other physical quantities – mechanical (strain, pressure), temperature, chemical (concentration and presence of gases and liquids).

A number of such sensors have been developed [8–12]. These sensors usually enable remote and accurate measurements of selected physical quantities. However, in some situations, their limitations appear: some of them use mechanical solutions (vulnerable to vibration) [12, 13], other sensors require a very complex micro-resonator structure [9–11] or the measurement range is relatively small [14]. Moreover, in some cases, an excitation with laser radiation in the free space is required, as well as very careful adjusting the measurement setup [15, 16]. Another common problem in measurement systems using fibre-optic sensors is the possibility of an accidental attenuation of the optical path, that translates into errors of the measured value (optoelectronic intensity sensors) [13, 17–19]. This is crucial, especially in the case of long optical paths connecting the sensor with the rest of the setup. There are few types of fibre optic sensors in which the impact of attenuation can be minimized: sensors using changes in fluorescence decay time and sensors that use changes of spectra in the optical signal. The latter group includes white light fibre-optic interferometers, called also low-coherence fibre-optic interferometers. They are characterized by small dimensions of a modulator (its thickness can be smaller than $0.5\ \mu m$), high resolution, high sensitivity and wide dynamic range. Moreover, they enable direct measurement of absolute values of measured quantities. In these sensors, the information about a measured value is encoded in the spectrum of the optical signal [20, 21]. Therefore, any changes in the intensity of the optical signal due to the change in the transmission of the optical link do not affect the measured signal spectrum.

In this work, we applied low-coherence interferometry to design a simple, low-cost fibre-optic sensor for accurate, simultaneous measurements of refractive index and thickness of liquid layers. Our construction uses an extrinsic fibre-optic *Fabry–Pérot interferometer* (FPI) as the optical signal modulator. There are many sensors that use this type of modulator; however, they often require a complex procedure of manufacturing an FPI cavity [22, 23]. The design of sensor head proposed in this paper uses commercially available components, not requiring any modification of the fibre.

The innovative solution implemented in the presented research is a combination of two light sources and only one sensing head operating at the same time. The use of two light sources enables to obtain complex and comprehensive information from two different spectral ranges. As a consequence, we can perform precise and accurate simultaneous measurements of both thickness and refractive index of a sample. Knowing these two values, we can determine the type of liquid and its thickness within a tenth of a micrometre [24].

2. Measurements and methods

2.1. Experimental setup

In order to measure refractive index and thickness of liquid layers we have designed an experimental low-coherence setup with a Fabry–Pérot sensing interferometer. The basic configuration of the measurement setup is shown in Fig. 1. It consists of an optical spectrum analyser (OSA, Yogokawa AQ6319, Japan) as the optical signal processor, two super-luminescent diodes

(Superlum Broad-lighter S1300-G-I-20, Ireland, Gaussian spectral density, central wavelength λ_{max} = 1290 nm, FWHM $\Delta\lambda_{FWHM}$ = 50 nm and Superlum Broad-lighter S1550-G-I-10, Ireland, Gaussian spectral density λ_{max} = 1560 nm, $\Delta\lambda_{FWHM}$ = FWHM) as the optical radiation source, a single mode (SMF-28) 2:1 fibre coupler, and a fibre-optic FPI as the sensing interferometer.
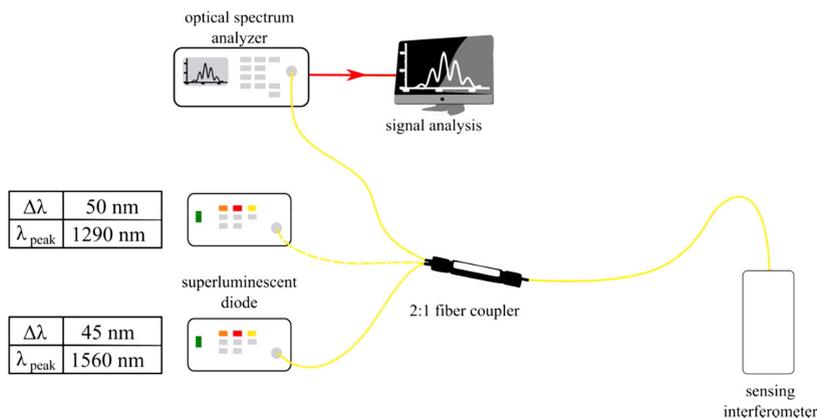

Fig. 1. Low-coherence measurement setup.

2.2. Sensing head

In the measurement setup presented in Fig. 1 the fibre-optic sensor with the extrinsic Fabry–Pérot cavity placed at the end of a single-mode fibre is used as the sensing interferometer. In the fibre-optic configuration of the FPI presented in Fig. 2 one of the mirrors is surface S_1 – a boundary layer between the polished end of the silica optical fibre and the Fabry–Pérot cavity, and the second mirror is surface S_2 – a boundary layer between the Fabry–Pérot cavity and the silver mirror (Thorlabs PFSQ10-03-P01).
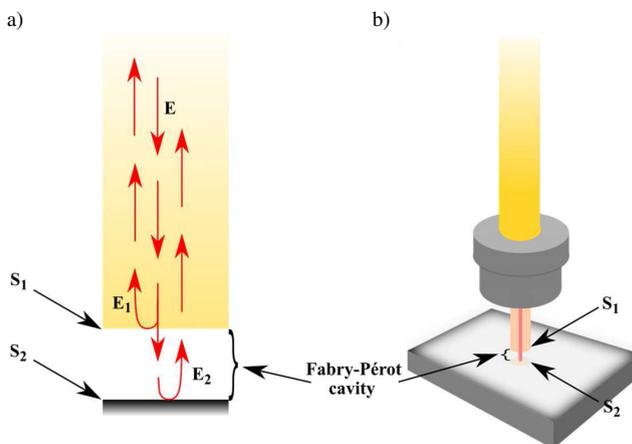

Fig. 2. Extrinsic fibre-optic Fabry-Pérot interferometer: a) beam propagation inside the interferometer cavity; b) a 3D view of the laboratory prototype. Description: E_1, E_2 – interfering beams, E – sum of interfering beams, S_1, S_2 – mirroring surfaces.

The FPI is a multi-beam interferometer. When it is illuminated by a plane wave, the intensity of both transmitted and reflected waves can be described by well-known Airy functions [25]. However, for the fibre-optic sensors with an extrinsic FPI, a two-beam model can be employed which is shown in Fig. 2a. The analysis of the signal was fully described in previous works, *e.g.* [26].

2.3. Measurements

We have performed several series of measurements on the designed experimental setup. The first stage was to perform measurements by expanding the cavity from 50 μm to 500 μm with a 50 μm step. The value of refractive index inside the cavity was constant and was equal to $n = 1.00$. The cavity width was controlled by a micrometre screw. Fig. 3 presents examples of spectra registered during this part of the experiment.
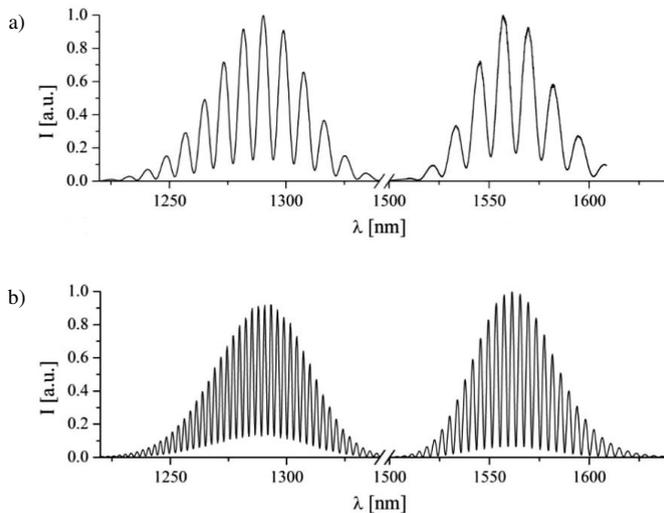

Fig. 3. Spectra registered during measurements for two light sources (spectra ranges: 1220÷1340 nm and 1500÷1640 nm) of an air-filled cavity ($n = 1.00$) of a width of: a) 100 μm; b) 300 μm.

As can be seen from Fig. 3, the wider FPI cavity, the smaller the distance between adjacent maxima, and hence the greater the number of maxima within the studied spectrum.

After careful examination of how the width of air-filled cavity affects the measurement signal spectrum, measurements of refractive index of several samples were performed. Liquid samples of known refractive indices were measured by filling the 200 μm wide fibre-optic FPI cavity. The measured refractive indices varied from 1.00 to 1.37. Fig. 4 presents examples of spectra of water and methanol recorded during measurements of refractive indices.

It can be noted that, as the refractive index increases, the spectrum changes. As a consequence, the distribution of spectral fringes in a specified spectrum range changes. Based on the performed initial research, we can certainly say that the presented measurement method is sensitive to the changes in both the substance refractive index and its layer thickness. A proper method of data analysis enables to determine these parameters' values in a single measurement, using only one measurement head.
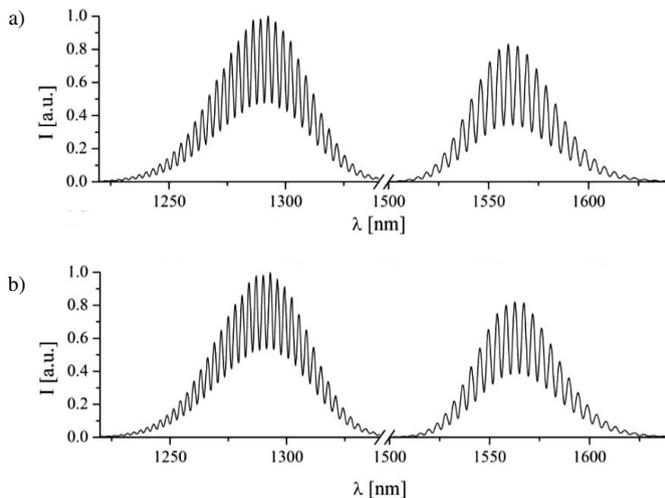
a)

b)

Fig. 4. Spectra registered during measurements (spectra ranges: 1220÷1340 nm and 1500÷1640 nm) of refractive indices, where cavity width was 200 μm. The examined substances were: a) methanol ($n = 1.30$); b) water ($n = 1.32$).

3. Results and discussion

3.1. Results of measurement of refractive index and thickness of liquid layers

The measurements were carried out with the use of two super-luminescent diodes. The spectra in a range of 1220÷1340 nm have been analysed to determine the refractive index of examined liquid (RI), and the spectra in a range of 1500÷1640 nm – to determine the liquid film thickness. Calibration curves (see Figs. 5–6) were determined for the measurements of both refractive index and layer thickness.
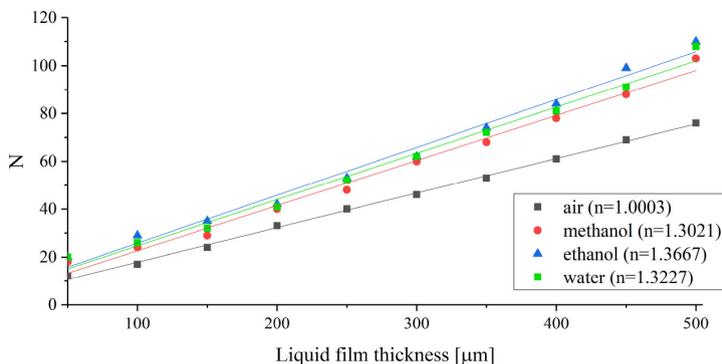

Fig. 5. Calibration curves for the measurements of refractive index. N – the number of maxima in the measurement signal spectrum.

The measurement data have been approximated using a linear function (see Figs. 5–6), and the values of determination coefficient R^2 have been calculated. R^2 coefficient describes the matching degree of the applied mathematical model to the measurement data and takes values from 0 to 1.
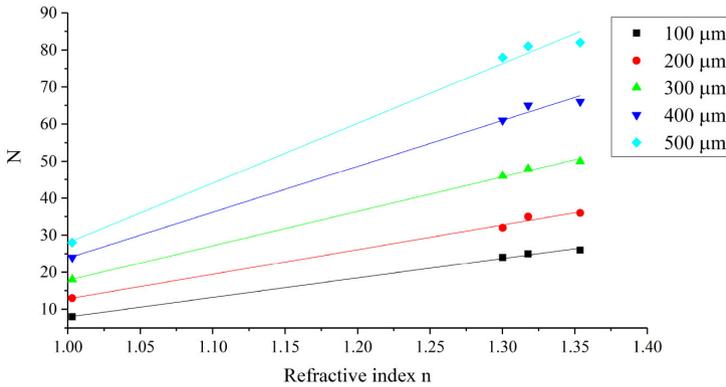
Fig. 6. Selected calibration curves for the measurements of liquid film thickness. N – the number of maxima in the measurement signal spectrum.

For the performed measurements, the values of the determination coefficient R^2 exceed 0.98 which means that the applied model very well matches the measurement data.

To determine liquid film parameters, the distribution of spectral fringes in the measurement signal spectrum must be known for two spectral ranges. For a particular distribution of spectral fringes only a few sets of parameters could be found, *e.g.* for the number of maxima in the measurement signal spectrum $N = 78$ in a wavelength range $1220 \div 1340$ nm the RI value of the examined liquid can be equal to 1.0003 (air; 516 µm film thickness), 1.3021 (methanol; 394 µm film thickness) or 1.3667 (ethanol; 361 µm film thickness), whereas for $N = 61$ in a wavelength range $1500 \div 1640$ nm the liquid film thickness values can be equal to 400 µm (for RI = 1.30 which is methanol), 450 µm (for RI = 1.25) and 500 µm (for RI = 1.21).

Comparison of the parameter sets for two wavelength ranges enables to find exact values of liquid film parameters. For the aforementioned example, the liquid film thickness is equal to 394 µm (the examined liquid is methanol); the result of examination is very close to the real parameter value 400 µm for a methanol film. The approximation-relative error, defined as magnitude of the difference between the exact value of parameter and its approximation divided by magnitude of the exact value of parameter, is expressed by (1):

$$\eta = \left| \frac{v - v_{approx}}{v} \right| \cdot 100\%. \tag{1}$$

In this case, the approximation-relative errors for liquid film thickness and RI of liquid are equal to 1.54% and 0.35%, respectively. These insignificant values of errors justify using the proposed method of RI and liquid layer thickness determination. Moreover, such very high accuracy can be obtained using a very simple and fast data analysis method.

3.2. Measurement resolution

In this paper, our goal was to apply a simple and fast data analysis method. For this reason, the maxima in the measurement spectra were counted and *N* means the number of maxima in the measurement signal spectrum.

The measurement resolution depends on a few factors. First, it depends on the employed optical spectrum analyser resolution. The increasing measurement resolution enables to detect signal changes in a more accurate way. During the described experiment, we performed measurements

with a 0.2 nm wavelength step. Secondly, it depends on the capabilities of validation method. In our setup, it is limited by the interferometer cavity length and the *refractive index* (RI) value accuracy. The interferometer cavity length was changed with a micrometric screw which resolution was 10 μm. Therefore, using this setup it is impossible to obtain cavity length measurement resolution better than 10 microns.

It should be mentioned, that more sophisticated spectrum analysis methods, *e.g.* [24], enable to improve the determination of examined liquid layer parameters.

4. Conclusion

In this paper, we present a remote fibre-optic sensor for simultaneous measurement of refractive index and thickness of a liquid layer. The measurement data have been approximated using a linear function with a very good determination coefficient R^2 – more than 0.98. The approximation-relative errors of measurements of liquid layer thickness and refractive index of liquid are equal to 1.54% and 0.35%, respectively.

The presented results show the unique capabilities of the developed sensor: 1) very precise measurement of refractive index and thickness of liquid layers; 2) possibility of relatively easy implementation of a sensor network, using several sensing heads; 3) possibility to repair a damaged optical fibre in a relatively easy way (standard optical fibres, easy to connect by splicing), without a need to re-calibrate the sensor.

Acknowledgements

References

[1] Bogdanowicz, R., Sobaszek, M., Ficek, M., Gnyba, M., Ryl, J., Siuzdak, K., Bock, W.J., Smietana, M. (2015). Opto-Electrochemical Sensing Device Based on Long-Period Grating Coated with Boron-Doped Diamond Thin Film. *J. Opt. Soc. Korea*, 19(6), 705–710.

[2] Jędrzejewska-Szczerska, M., Karpienko, K., Wróbel, M.S., Tuchin, V.V. (2016). Sensors for Rapid Detection of Environmental Toxicity in Blood of Poisoned People, in: Nikolelis D., Nikoleli GP. (eds). *Biosensors for Security and Bioterrorism Applications. Advanced Sciences and Technologies for Security Applications*. Cham: Springer.

[3] Wierzba, P., Jędrzejewska-Szczerska, M. (2013). Optimization of a Fabry-Perot Sensing Interferometer Design for an Optical Fiber Sensor of Hematocrit Level. *Acta Phys. Pol. A.*, 114(6-A) A-127–A-131.

[4] Hirsch, M., Majchrowicz, D., Wierzba, P., Weber, M., Bechelany, M., Jędrzejewska-Szczerska, M. (2017). Low-Coherence Interferometric Fiber-Optic Sensors with Potential Applications as Biosensors. *Sensors (Basel)*, 17(2), 261-1–216-12.

[5] Yin, M., Gu, B., An, Q.-F., Yang, C., Guan, Y.L., Yong, K.-T. (2018). Recent development of fiber-optic chemical sensors and biosensors: Mechanisms, materials, micro/nano-fabrications and applications, Coord. *Chem. Rev.*, 376, 348–392.

[6] Yhuwana, Y.G.Y., Apsari, R., Yasin, M. (2017). Fiber optic sensor for heart rate detection. *Optik (Stuttg)*, 134, 28–32.

[7] Kaushik, S., Pandey, A., Tiwari, U.K., Sinha, R.K. (2018). A label-free fiber optic biosensor for Salmonella Typhimurium detection. *Opt. Fiber Technol.*, 46, 95–103.

[8] Selvas-Aguilar, R., Castillo-Guzman, A., Cortez-Gonzalez, L., Toral-Acosta, D., Martinez-Rios, A., Anzueto-Sanchez, G., Duran-Ramirez, V.M., Arroyo-Rivera, S. (2016). Noncontact Optical Fiber Sensor for Measuring the Refractive Index of Liquids. *J. Sensors 2016*, 3475782-1–3475782-6.

[9] Boleininger, A., Lake, T., Hami, S., Vallance, C., Boleininger, A., Lake, T., Hami, S., Vallance, C. (2010). Whispering Gallery Modes in Standard Optical Fibres for Fibre Profiling Measurements and Sensing of Unlabelled Chemical Species. *Sensors*, 10(3), 1765–1781.

[10] Chiang, C.C., Chao, J.-C. (2013). Whispering Gallery Mode Based Optical Fiber Sensor for Measuring Concentration of Salt Solution. *J. Nanomater.*, 372625-1–372625-4.

[11] Knittel, J., Swaim, J.D., McAuslan, D.L., Brawley, G.A., Bowen, W.P. (2013). Back-scatter based whispering gallery mode sensing. *Sci. Rep.*, 3, 29741-1–2974-5.

[12] Kuang, J.-H., Chen, P.-C., Chen, Y.-C., Chen. (2010). Plastic Optical Fiber Displacement Sensor Based on Dual Cycling Bending. *Sensors*, 10(11) 10198–10210.

[13] Wu, Q., Semenova, Y., Wang, P., Hatta, A.M., Farrell, G. (2011). Experimental demonstration of a simple displacement sensor based on a bent single-mode–multimode–single-mode fiber structure. *Meas. Sci. Technol.*, 22(2), 025203-1–025203-5.

[14] Miao, Y., Li, C., Ma, X., Yao, J. (2016). Refractive index sensor based on thin-core microfiber. *15th Int. Conf. Opt. Commun. Networks*, 1–3.

[15] Zhang, L., Zhang, Z., Wang, Y., Ye, M., Fang, W., Tong, L. (2017). Optofluidic refractive index sensor based on partial reflection. *Photonic Sensors*, 7(2), 97–104.

[16] Selvas-Aguilar, R., Castillo-Guzman, A., Cortez-Gonzalez, L., Toral-Acosta, D., Martinez-Rios, A., Anzueto-Sanchez, G., Duran-Ramirez, V.M., Arroyo-Rivera, S. (2016). Noncontact Optical Fiber Sensor for Measuring the Refractive Index of Liquids. *J. Sensors 2016*, 3475782-1– 3475782-6.

[17] Kim, C.-B., Su, C.B. (2004). Measurement of the refractive index of liquids at 1.3 and 1.5 micron using a fibre optic Fresnel ratio meter. *Meas. Sci. Technol.*, 15(9), 1683–1686.

[18] Xiumei, G., Yanping, L., Luansheng, J., Chongxiao, M. (2012). The Design of Optical Fiber Displacement Sensor System, W. Zhang (ed.). *Software Engineering and Knowledge Engineering: Theory and Practice. Advances in Intelligent and Soft Computing*, Berlin, Heidelberg: Springer Berlin Heidelberg.

[19] Ma, Y., Farrell, G., Semenova, Y., Chan, H.P., Wu, Q. (2012). High sensitivity refractive index sensor based on multimode fiber coated with an axisymmetric metal grating layer. *2012 Asia Commun. Photonics Conf.*, AF4B.7-1– AF4B.7-3.

[20] Jedrzejewska-Szczerska, M. (2008). Improved Methods of Signal Processing Used in Low-Coherent Systems. *Acta Phys. Pol. A.*, 114(6–A),127–131.

[21] Grattan, K.T.V., Meggitt, B.T. (2000). *Optical Fiber Sensor Technology: Fundamentals.* Boston: Springer, US.

[22] Rao, Y.-J. (2006). Recent progress in fiber-optic extrinsic Fabry-Perot interferometric sensors. *Opt. Fiber Technol.*, 12(3), 227–237.

[23] Islam, M., Ali, M., Lai, M.-H., Lim, K.-S., Ahmad, H., (2014). Chronology of Fabry-Perot Interferometer Fiber-Optic Sensors and Their Applications: A Review. *Sensors.*, 14(4), 7451–7488.

[24] Pluciński, J., Karpienko, K. (2016). Fiber optic Fabry–Pérot sensors: modeling versus measurements results. *Proc. SPIE 10034*, Szczyrk, Poland, 100340H-1–100340H-7.

[25] Born, M., Wolf, E., Bhatia, A.B., Clemmow, P.C., Gabor, D., Stokes, A.R., Taylor, A.M., Wayman, P.A., Wilcock, W.L. (1999). *Principles of Optics: Electromagnetic Theory of Propagation, Interference and Diffraction of Light*. Cambridge: Cambridge University Press.

[26] Jedrzejewska-Szczerska, M., Bogdanowicz, R., Gnyba, M., Hypszer, R., Kosmowski, B.B. (2008). Fiber-optic temperature sensor using low-coherence interferometry. *Eur. Phys. J. Spec. Top.*, 154(1), 107–111.